Biomech Model Mechanobiol (2012) 11:49–59
DOI 10.1007/s10237-011-0292-4

ORIGINAL PAPER

A three-dimensional random network model of the cytoskeleton and its role in mechanotransduction and nucleus deformation

Yukai Zeng · Ai Kia Yip · Soo-Kng Teo · K.-H. Chiam

Received: 26 July 2010 / Accepted: 25 January 2011 / Published online: 10 February 2011

Abstract We have developed a three-dimensional random network model of the intracellular actin cytoskeleton and have used it to study the role of the cytoskeleton in mechanotransduction and nucleus deformation. We use the model to predict the deformation of the nucleus when mechanical stresses applied on the plasma membrane are propagated through the random cytoskeletal network to the nucleus membrane. We found that our results agree with previous experiments utilizing micropipette pulling. Therefore, we propose that stress propagation through the random cytoskeletal network can be a mechanism to effect nucleus deformation, without invoking any biochemical signaling activity. Using our model, we also predict how nucleus strain and its relative displacement within the cytosol vary with varying concentrations of actin filaments and actin-binding proteins. We find that nucleus strain varies in a sigmoidal manner with actin filament concentration, while there exists an optimal concentration of actin-binding proteins that maximize nucleus displacement. We provide a theoretical analysis for these nonlinearities in terms of the connectivity of the random cytoskeletal network. Finally, we discuss laser ablation experiments that can be performed to validate these results in order to advance our understanding of the role of the cytoskeleton in mechanotransduction.

Keywords Cytoskeleton · Random network model · Mechanotransduction · Nucleus deformation

Y. Zeng · A. K. Yip · S.-K. Teo · K.-H. Chiam (✉)
A*STAR Institute of High Performance Computing,
1 Fusionopolis Way #16-16, Singapore 138632, Singapore
e-mail: chiamkh@ihpc.a-star.edu.sg

K.-H. Chiam
Mechanobiology Institute, National University of Singapore,
5A Engineering Drive 1 #05-01, Singapore 117411, Singapore

1 Introduction

Cells are constantly being subjected to mechanical stresses arising from their interactions with the environment. These mechanical stresses are known to cause changes in intracellular biochemistry and gene expression (Lo et al. 2000; Dalby et al. 2004; Guo et al. 2006; Na et al. 2008). For example, the differentiation of mesenchymal stem cells into different lineages can be controlled by the substrate stiffness (an extracellular mechanical signal) on which these cells are cultured on (Engler et al. 2006). The mechanisms converting mechanical signals into downstream biochemical signals, generically termed "mechanotransduction," are an active area of study. In this paper, we focus on a specific form of mechanotransduction: the direct transmission of stresses from the cell exterior to the nucleus. The exact mechanisms of this process are still not well characterized. This is to be contrasted to the many other examples of mechanotransduction that have been relatively well studied. For example, mechanosensitive ion channels on the cell membrane convert mechanical signals, in the form of membrane stretch, into electrical and/or chemical signals to regulate ion flux across the cell membrane (Martinac 2004). Transmembrane proteins such as G-proteins (Gudi et al. 1998; Mederos y Schnitzler et al. 2008), protein kinases such as p130CAS and Src (Giannone and Sheetz 2006; Chien 2007), and cell-matrix adhesion proteins such as integrins, PECAM1 and cadherins (Tzima et al. 2005; Liu et al. 2007; Tetsunaga et al. 2009) are also known to be activated by mechanical forces, which can then trigger downstream signaling cascades, leading to changes in gene expressions (Wang et al. 2009).

There have been experiments that looked at nucleus deformation (Maniotis et al. 1997) as a "marker" for mechanotransduction. These experiments have shown that by applying stresses on cell surface receptors such as integrins,

nucleus deformation can be induced (Maniotis et al. 1997). On the other hand, cells treated with cytoskeleton-disrupting drugs such as cytochalasin D did not show significant nucleus deformation. This suggests that the cell cytoskeleton could play an important role in transmitting forces directly to deform the nucleus. However, it is plausible that nucleus deformation can be triggered biochemically. In such a scenario, mechanical stresses applied to the plasma membrane propagate to the cytoskeleton, causing it to remodel which in turn triggers certain signaling cascades to up- or downregulate certain signaling molecules. These signaling molecules diffuse into the nucleus and activate processes that change the nucleus shape (such as the polymerization or depolymerization of the nucleoskeleton filaments (Nalepa and Harper 2004) or restructuring of the lamin network). However, this has not been shown definitively. Therefore, we do not consider biochemical signaling triggered by force-induced activation of cell membrane proteins in this paper, but instead show that mechanical coupling can be a mechanism for mechanotransduction. The plasma membrane is coupled to the cytoskeleton via focal adhesion complexes that are bound to membrane receptors such as integrins. The focal complexes are in turn coupled to the actin filaments. The cytoskeleton couples to the nucleus membrane via proteins containing the Sad1/UNC-84 (SUN) and Klarsicht/ANC-1/Syne-1 homology (KASH) domains. These proteins are members of the linkers of the nucleoskeleton to the cytoskeleton (LINC) complexes, a family of macromolecular assemblies that span the double membrane of the nuclear envelope (Crisp et al. 2006). These connections form a mechanically coupled system connecting the nucleus membrane to the plasma membrane. Thus, forces applied to the cell surface can be transmitted through the cytoskeleton to the nucleus and cause it to deform (Maniotis et al. 1997). This change in nucleus shape may lead to changes in nucleus structure and gene expression (Thomas et al. 2002).

To this end, we develop a three-dimensional random network model of the cytoskeleton and use it to show that mechanical coupling of this random cytoskeleton network to both the plasma membrane and the nucleus membrane can be a plausible mechanism for mechanotransduction. This mechanical coupling between the plasma membrane, cytoskeleton, and nucleus membrane allows for stress propagation to occur in the range of seconds (Na et al. 2008), compared to biochemical signaling which is likely to be diffusion limited and occurs typically in the range of minutes or longer.

Our model for the three-dimensional random cytoskeletal network represents the cytoskeleton by two sets of randomly distributed linear Hookean springs. The first set of springs represents the actin filaments, while the second set represents the actin-binding proteins that connect the filaments. The actin filaments are attached to the plasma and nucleus membranes at random points. These two membranes are represented as deformable neo-Hookean membranes. We have neglected the contributions of microtubules and intermediate filaments. The former is known to bear only compressive stresses and not tensile stresses. However, the compressive stresses generated in our random network are expected to be small, and so the contributions of microtubules will be small. The latter contributes to mechanical stability of the cell only at high tensile stresses, which are not expected from our extent of mechanical perturbations. Jean et al. (2005) proposed an axisymmetric finite element model to show how changes in cytoskeleton tension during cell rounding from an adhered state can change the nucleus shape. In their model, the cytoskeleton network is represented by either discrete fibers or an effective homogenous layer that connects the nucleus to the adhesion sites. However, their model is insufficient because it assumes idealized cell geometries and neglects the random connectivity of the cytoskeleton network. Shafrir and Forgacs (2002) proposed a two-dimensional model of the cytoskeleton as a random network of rigid rods representing the actin filaments and linear Hookean springs representing the actin crosslinkers. However, they assumed that the plasma and nucleus membranes are rigid and immobile, which is unrealistic. In this paper, we have modeled the actin network as a random connected network of linear springs. This is a simplified representation compared to other more sophisticated models (Head et al. 2003; Onck et al. 2005; Huisman et al. 2007; Palmer and Boyce 2008; Kim et al. 2009). However, these more sophisticated models are focused on understanding the rheology of the actin network. Connecting these network models to the plasma and nuclear membranes is not straightforward. In addition, our model allows us to study the effects of the flexibility of the cross-linking proteins. This effect is not considered in the models of Head et al. (2003), Onck et al. (2005), Huisman et al. (2007) as they assumed the cross-links between the actin filaments to be rigid. However, there are many examples of flexible cross-linking proteins, such as filamin, and it has been shown that the response of network that is cross-link by filamin more closely mimics the mechanical properties of cells (Gardel et al. 2006a,b). Although the model proposed by Kim et al. (2009) takes into account the flexibility of the cross-linking proteins, the computational demands of its Brownian dynamics, it is less suited for studying the effects of mechanical coupling between the cytoskeleton and the plasma and nucleus membranes. The length scale of this mechanical coupling, which is of interest in this paper, is approximately 10 μm and is significantly larger than the computational domain described in their approach.

The remaining of this paper is organized as follows. In Sect. 2, we describe the formulation of our model and the numerical techniques used to solve it. In Sect. 3, we first validate our model by measuring the strain and displacement

of the nucleus when an external pulling force is applied to part of the plasma membrane and comparing the results to the experimental results of Maniotis et al. (1997). We then study the effects of increasing the concentrations of actin filaments and actin-binding proteins on nucleus strain and displacement under the same external loading. In Sect. 4, we discuss these results in the context of the network connectivity and provide a theoretical justification for the results we observed. We also discuss how our model can be applied to other experimental scenarios and suggest experiments that can be performed to validate our model. Finally, in Sect. 5, we present our conclusions.

2 Methods

The cytoskeleton is modeled as two sets of linear Hookean springs, one representing actin filaments and the other representing actin- binding proteins, randomly distributed and connected to form a three-dimensional random network. A schematic is shown in Fig. 1. To generate the initial configuration of the cytoskeleton network, actin springs with lengths randomly chosen from the range 3.5 to 4 μm are randomly distributed in the region between the plasma and nucleus membranes. Springs that intersect other spring(s) are discarded. Springs that intersect the cell or nucleus membranes are truncated and attached to the nearest membrane nodal point. These attachment points represent the mechanical coupling between the cytoskeleton and the cell/nucleus membranes. In our model, the linear spring representation of the actin filaments can be seen as a useful simplification of the nonlinear force-extension constitutive model of single actin filaments such as that derived in Palmer and Boyce (2008). The constitutive model of a single actin filament in that paper incorporates the straightening of bends in the fluctuating filament under an external axial force. In their model, in the absence of any external applied axial force, the end-to-end distance of the filament is less than its contour length as a result of thermal fluctuation. The application of an external axial force causes the filament to straighten, and the resultant force-extension response can be approximated by a nonlinear function that incorporates strain stiffening. The strain-stiffening response can be understood in terms of the increased entropic resistance as the length of the filament approaches its contour length. In our model, the initial length of the actin filaments can be viewed as the end-to-end distance of a bend fluctuating filament, rather than the filament contour length. Hence, our linear spring model approximates the initial force-extension of the actin filament prior to the onset of strain stiffening. However, we do note that a densely cross-linked network (where the filament persistence length $\geq$ contour length) operates in the highly nonlinear regime of this force-extension curve. Thus, the linear

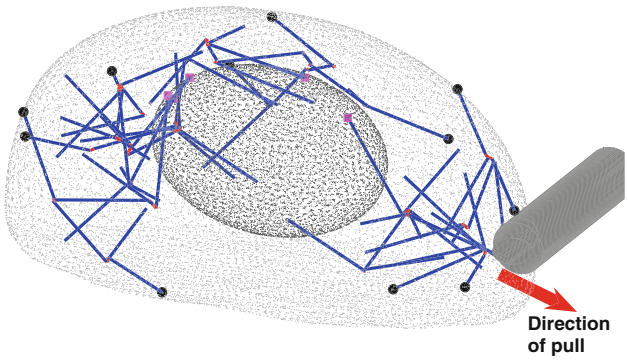

Fig. 1 Schematic of the three-dimensional random cytoskeleton network, with actin filaments shown in *blue* and actin-binding proteins shown in *red*. *Black circles* and *magneta squares* represent anchor points between the actin springs and the plasma membrane and nucleus membrane, respectively. The micropipette attached to the cell membrane is pulled away from the cell to induce an external loading

force-extension of the actin filaments in our model should strictly be viewed as a simple and useful approximation to the more realistic albeit more complex force-extension response derived in Palmer and Boyce (2008). In addition, our cytoskeleton network model is capable of accommodating nonaffine deformations through both rotation and stretching of the spring elements representing actin filaments and actin-binding proteins. In this manner, the addition degrees of freedom associated with the rotation of these elements in the network allow the applied mechanical stress to be borne without those elements aligned in the direction of the applied stress being excessively stretched (Palmer and Boyce 2008). This further supports the simplification made in the choice of the linear force-extension response for the actin filaments in our model. Despite the simplicity of our model, it is still able to retain the key features of the cytoskeleton network in a qualitative manner and to improve our understanding of the effect of mechanical coupling as the network connectivity is varied.

The springs representing the actin-binding proteins (hereafter referred to as linker springs) connect to the ends of any two actin springs if the distance between these end points is less than a specified cutoff length. This cutoff length therefore determines the number of linker springs. The larger the cutoff, the more linker springs there will be. For example, for a cutoff length of 200 nm which is the typical dimension of filamin (Alberts et al. 2002), a total of 5,176 linker springs will be generated, corresponding to a crosslinker concentration of 0.5 mg/ml. The number of actin springs N_a is set to be approximately 16,000 which corresponds to an actin filament concentration of approximately 1.56 mg/ml. The number of linker springs N_l is varied from 657 to 13372, corresponding to an actin-binding protein concentration range of 0.06–1.3 mg/ml. These values are consistent with values used in in-vitro reconstituted actin network studies (Shin et al. 2004). The rest lengths of the springs are set to be their original lengths as initialized. They are assumed to be linear and

follow Hooke's law. The stiffness of the actin and linker springs is $k_a = 1$ pN/μm and $k_l = 0.1$ pN/μm, respectively (Shafrir and Forgacs 2002). The springs are immersed in a viscous medium representing the cytosol, whose viscosity we set as $\eta = 1$ cP (Mastro et al. 1984). The displacement of the springs as they stretch or contract is opposed by viscous drag. Force balance then yields the following equation of motion for the three-dimensional positions of the ends of the actin springs, $\mathbf{x}_{ij}$, where the subscript denotes the ith end of the jth spring with $i = 1, 2$ denoting one of the two ends and $j = 1, \ldots, N_a$,

$$k_a(|\mathbf{x}_{1j} - \mathbf{x}_{2j}| - a_j)\hat{d}_j + \sum_{i',j'} k_l(|\mathbf{x}_{ij} - \mathbf{x}_{i'j'}| - l_{iji'j'})\hat{d}_{iji'j'} + \eta\frac{d\mathbf{x}_{ij}}{dt} = 0. \quad (1)$$

Here, a_j denotes the rest length of the jth actin spring and $\hat{d}_j = (\mathbf{x}_{1j} - \mathbf{x}_{2j})/|\mathbf{x}_{1j} - \mathbf{x}_{2j}|$ is a unit vector specifying its orientation. The sum in the second term is over (i', j') if the ith end of the jth actin spring is connected to the i'th end of the j'th actin spring by a linker spring, and $l_{iji'j'}$ is the rest length of that linker spring. Similarly, $\hat{d}_{iji'j'} = (\mathbf{x}_{ij} - \mathbf{x}_{i'j'})/|\mathbf{x}_{ij} - \mathbf{x}_{i'j'})$ is a unit vector specifying the orientation of that linker spring.

The initial shape of the plasma membrane is arbitrarily chosen to be like that of an adhered cell spreading on a flat substrate with length along its major axis $D = 30$ μm. The initial shape of the nucleus membrane is arbitrarily chosen to be an oblate spheroid with equatorial diameter $d = 13$ μm. See Fig. 1. Both membranes are discretized into triangular elements that can deform by stretching and bending and whose displacements are opposed by viscous drag and, for those elements with actin springs attached, pulling from the displacement of the actin springs. In addition, the mechanical properties of the shell-like actin cortex found underneath the plasma membrane are incorporated into that of the plasma membrane. If $\mathbf{u}$ denotes the three-dimensional displacement of a node of a triangular mesh of the membrane in the global coordinate system, $\mathbf{v}$ the two-dimensional in-plane displacement, and $\mathbf{u} = \mathbf{T}\mathbf{v}$ with $\mathbf{T}$ the transformation matrix, then force balance yields

$$\mathbf{T}\frac{\partial W_s}{\partial \lambda_i}\frac{\partial \lambda_i}{\partial \mathbf{v}} + \frac{\partial W_b}{\partial \phi}\frac{\partial \phi}{\partial \mathbf{u}} + \mathbf{f}_s + \eta\frac{\mathrm{d}\mathbf{u}}{\mathrm{d}t} = 0. \quad (2)$$

Here, $W_{s,b}$ are the strain energy functions for stretching and bending, respectively, $\lambda_{1,2}$ the in-plane principal strains, ϕ the dihedral angle between adjacent elements (Marcelli et al. 2005), and $\mathbf{f}_s$ the force resulting from the pulling of actin springs, if any (calculated from the first two terms of Eq. 1). The strain energy function for stretching is assumed to be neo-Hookean,

$$W_s = \frac{E_s}{6}(\lambda_1^2 + \lambda_2^2 + \lambda_1^{-2}\lambda_2^{-2} - 3) + E_d(\lambda_1\lambda_2 - 1)^2, \quad (3)$$

with $E_{s,d}$ the membrane shear and area dilation modulus, respectively (Evans and Skalak 1979a,b). The strain energy function for bending is

$$W_b = \kappa(1 + \cos(\phi)), \quad (4)$$

where κ is the membrane bending modulus. This formalism is used for both the plasma membrane and the nucleus membrane. The values used for the plasma membrane shear and dilatation moduli are $E_{sp} = 0.006$ dyn/cm and $E_{dp} = 0.6$ dyn/cm, respectively. These values are consistent with those reported in literature for erythrocytes (Doddi and Bagchi 2009) and endothelial cells (Sato et al. 1987; Wiesner et al. 1997). The values used for the nucleus membrane shear and dilatation moduli are $E_{sn} = 6$ dyn/cm and $E_{dn} = 0.6$ dyn/cm, respectively. The values used for the bending moduli of the plasma and nucleus are assumed to be identical, $\kappa_p = \kappa_n = 6 \times 10^{-20}$ J (Marcelli et al. 2005).

In choosing the values of the shear and dilational moduli of the nuclear and plasma membranes, we considered the following points. First, the mechanical resistance of the nuclear membrane is reinforced by the presence of an underlying lamina network. The nuclear lamina network is a ∼ 10 -nm-thick protein meshwork associated with the inner nuclear membrane composed of lamins (Stewart et al. 2007). This protein meshwork therefore serves as a structural scaffold to the nuclear membrane, providing additional mechanical resistance to its shearing when compared to the plasma membrane. Thus, we would expect that the value for the shear modulus of the nuclear membrane to be significantly higher to reflect this mechanical reinforcement. Second, the dilational modulus in our membrane formulation is used to conserve the local surface area of the membrane elements, reflecting the local inextensibility of the membrane under mechanical stresses. Since the primary components of the nuclear and plasma membranes are identical, we have no *a priori* justifications to expect that this local inextensibility response will differ between the two sets of membranes. Thus, we would expect the dilation moduli of the nuclear and plasma membranes to be of the same value. Third, the contribution of bending resistance to the overall stiffness of the plasma membrane appears to be insignificant based on the reported values of the bending modulus in (Marcelli et al. 2005) (in the region of 10^{-20} J). Using a typical value of ∼ 10 nm for the plasma membrane thickness and a shear modulus of approximately 10^{-6} N/m, we estimate the energy attributed to shearing to be approximately in the region of 10^{-15} J. This is at least five orders of magnitude higher as compared to the contribution from bending. Thus, we would expect the choice of values for the bending moduli of the nuclear and plasma membranes to have minimal effects on our results. This justified our choice of assigning the value of the nuclear membrane bending modulus to be the same as that of the plasma membrane. (We acknowledge that it is

possible that the bending modulus of the nuclear membrane could be significantly higher when compared to the plasma membrane owning to the reinforcement effect of the lamina network. However, the contribution of the bending resistance will only be evident in the case of very sharp localized curvature change in the nuclear membrane. For our simulation setup, we do not expect such sharp curvature changes for the nuclear membrane to occur and this point further support our choice of assigning the same bending moduli for both the nuclear and plasma membranes.)

Taking the above points into consideration, we assign the value of the nuclear membrane shear modulus to be 1,000 times higher compared to that of the plasma membrane. Our nucleus model neglects any elastic contribution of the nuclear interior as it is represented by a viscous liquid in our formulation. Hence, the nucleus deformation is governed entirely by its membrane properties, namely the shear, dilation and bending moduli. It could be argued that the higher overall stiffness of the nucleus was achieved artificially given the unrealistically high value of the nuclear membrane shear modulus. However, we are interested only in studying the overall deformation of the nucleus as a result of the mechanical coupling from the cytoskeleton rather than the more detailed stress/strain distribution within the nucleus interior. Therefore, our simplified nucleus model is still justified as the higher nucleus stiffness (approximately an order of magnitude stiffer compared to the entire cell) is consistent with literature results and does not contradict the results from previous works (Caille et al. 2002). This "crude" presentation of the nucleus reduces the modeling complexity and computational costs in our formulation but still allows us to retain the key features governing the nucleus deformation.

We sought to justify the value of the nuclear membrane shear modulus by considering the contribution of the lamina network and nucleus prestress in our analysis. Yet, it is likely that the value of the nuclear membrane shear modulus is overestimated in our model owning to the absence of internal nucleus elasticity. We also acknowledge that it is also possible that the various moduli of the nuclear membrane are similar in values to the plasma membrane and that the difference in the stiffness between the nucleus and the entire cell reported experimentally can be attributed entirely to the interior elasticity of the nuclear contents (such as the highly compacted regions of chromosomes). This simplified nucleus representation of a membrane enclosing a viscous interior is one of the limitations of our model. However, this simplification is still valid and justified in the context of studying the deformation of the nucleus as a result of the cytoskeleton coupling.

A summary of these and other parameters of the model, and their values used in our simulations, is shown in Table 1. We have also verified that, qualitatively, our results are not sensitive to the exact values of these parameters.

Table 1 Parameters and their values used in the simulation

Parameter	Symbol	Value
Cell equatorial diameter	D	30 μm
Nucleus equatorial diameter	d	13 μm
Actin filament length	a	3.5–4 μm
Actin filament concentration	C_a	1.56 mg/ml
Number of actin springs	N_a	16000
Actin filament stiffness	k_a	1 pN/μm
Actin-binding protein stiffness	k_l	0.1 pN/μm
Actin-binding protein concentration	C_l	0.5 mg/ml
Number of linker springs	N_l	5176
Plasma membrane shear modulus	E_{sp}	0.006 dyn/cm
Plasma membrane dilatation modulus	E_{dp}	0.6 dyn/cm
Plasma membrane bending modulus	κ_p	6×10^{-20} J
Nucleus membrane shear modulus	E_{sn}	6 dyn/cm
Nucleus membrane dilatation modulus	E_{dn}	0.6 dyn/cm
Nucleus membrane bending modulus	κ_n	6×10^{-20} J
Cytosol viscosity	η	1 cP

3 Results

3.1 Model validation

We apply our model to simulate the experiment of (Maniotis et al. 1997), where a micropipette is pushed into the cytoplasm of a bovine capillary endothelial cell and then pulled away for a distance of either 10 or 20 μm at a rate of 5–10 μm/s. The strain and relative displacement of the nucleus were then measured by using real-time video microscopy. In our simulations, we model the micropipette pulling on the cytoskeleton by imposing a constant velocity of 5 μm/s on a subset of plasma membrane nodal points representing bounded integrin receptors being pulled by the micropipette; see Fig. 1. In Fig. 2, we show the results of our simulation of micropipette pulling. Panels (a–c) show the plasma and nucleus membranes at different time points of micropipette pulling, whereas panel (d) shows the cross-sectional view of the steady-state deformation of the plasma and nucleus membranes for pulling distances of 10 and 20 μm. The nucleus strain is defined as the ratio of the change in nucleus diameter in the direction of pull to its original diameter, calculated as (d'/d-1) and (d''/d-1) for pulling distances of 10 and 20 μm, respectively. The nucleus displacement is defined as the distance which the end of the nucleus furthest away from the rod has moved in the direction of the pull; it is denoted by x' and x'' for pulling distances of 10 and 20 μm, respectively. In Fig. 3, we plot these quantities obtained from our simulations and see that they compare well to the values reported in (Maniotis et al. 1997).

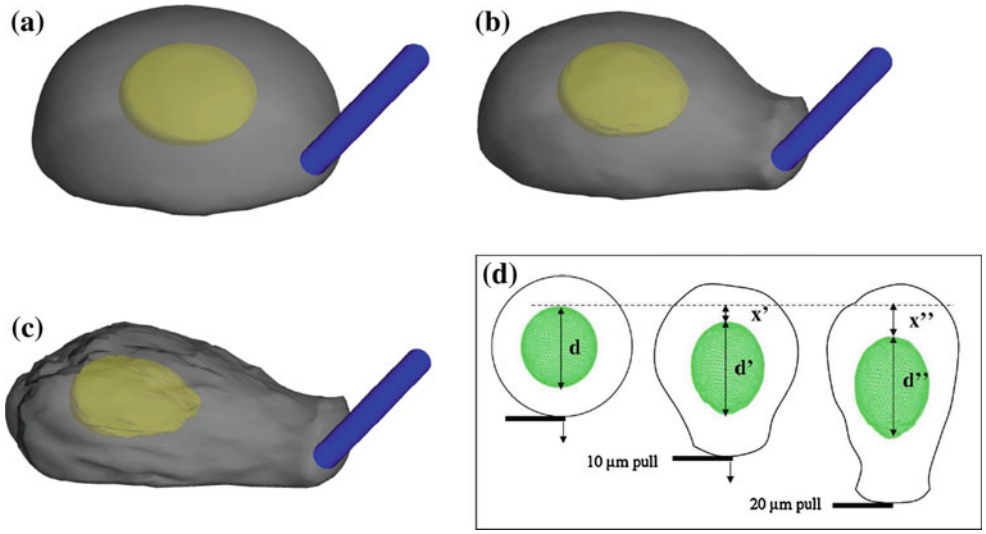

Fig. 2 Deformation of the plasma and nucleus membranes induced by micropipette pulling at different time points: **a** 0 s (initial unperturbed state), **b** 1 s, and **c** 25 s. The cytoskeleton network is omitted from these snapshots for clarity. **d** Cross-sectional view of the steady-state deformation of the plasma and nucleus membranes for different micropipette pulling distances of 10 and 20 μm. The nucleus diameter d is deformed to d' and d'', respectively, and displaced by x' and x'', respectively

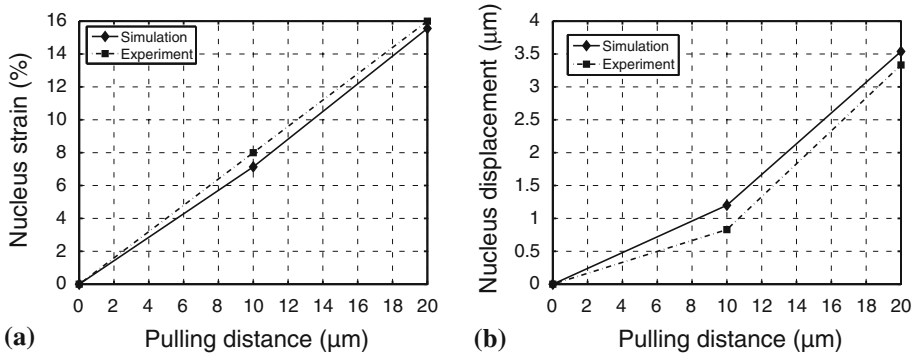

Fig. 3 **a** Nucleus strain and **b** nucleus displacement obtained from our simulations compared to the experiments of micropipette pulling on the cell surface (Maniotis et al. 1997)

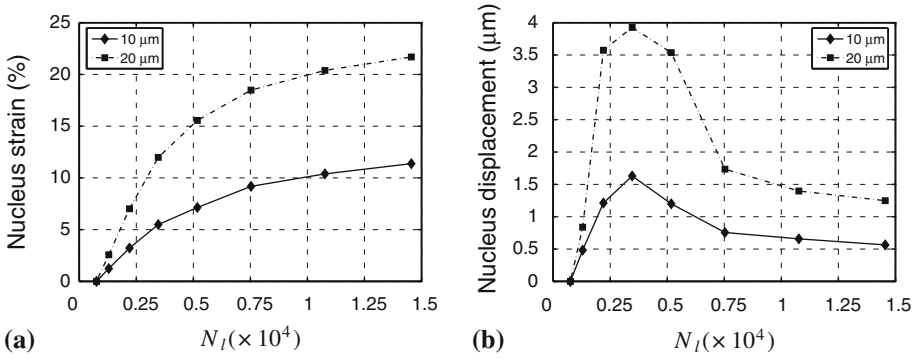

Fig. 4 **a** Nucleus strain and **b** nucleus displacement number of linker springs N_l at pulling to 10 μm (*solid lines*) and 20 μm (*dash-dot lines*). The number of actin springs is kept at $N_a = 1.6 \times 10^4$

3.2 Effects of varying network connectivity

We can numerically change the number of actin and linker springs and see how this change affects the ability of the random cytoskeleton network to act as a transducer of mechanical stress from the plasma membrane to the nucleus membrane. In Fig. 4, we show results from our simulations of how the nucleus strain and displacement change with changing the number of linker springs N_l for both pulling to 10 and 20 μm while keeping the number of actin springs N_a fixed. We see that there is a sigmoidal increase in the nucleus strain for increasing N_l for both pulling distances that plateau off at high N_l. On the other hand, the nucleus displacement exhibits a biphasic response with a maximum at $N_l \approx 3500$.

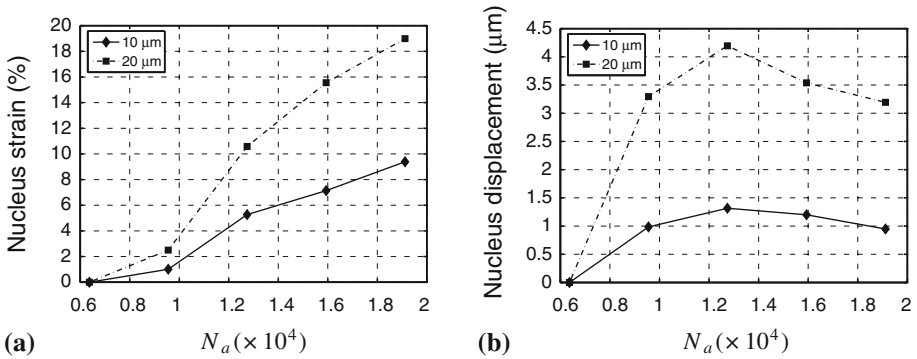

Fig. 5 **a** Nucleus strain and **b** nucleus displacement number of actin springs N_a at pulling to 10 μm (*solid lines*) and 20 μm (*dash-dot lines*). The number of linker springs also increases with N_a as described in the text

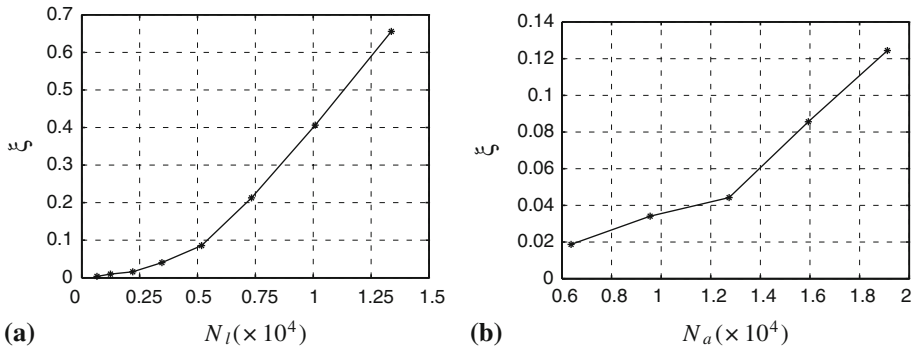

Fig. 6 Network connectivity ξ vs. **a** Number of linker springs N_l and **b** number of actin springs N_a. For panel (a), the number of actin springs is kept constant at $N_a = 1.6 \times 10^4$

Subsequently, increasing N_l leads to a nonlinear decrease in the nucleus displacement. We also note that both the nucleus strain and displacement become greater than zero at a value of N_l that is not zero; this threshold is approximately 660, corresponding to a concentration of actin-binding proteins of approximately 0.06 mg/ml. This suggests the existence of a percolation threshold for stress propagation through the cytoskeleton network. The role of percolation as a mechanism of mechanotransduction has been previously discussed (Forgacs 1995; Dalby 2005), in particular in the context of signal amplification, i.e., the number of localized mechanical perturbations increases as they percolate through the network from the plasma membrane to the nucleus membrane, but has never been measured experimentally.

In Fig. 5, we show results from our simulations of how the nucleus strain and displacement change with changing the number of actin springs N_a for both pulling to 10 and 20 μm. In these simulations, as N_a changes, N_l changes as well. This is because as the number of actin springs increases, the frequency of a linker spring being within the same cut-off distance within two ends of two actin springs increases. This simulates the physiological scenario that, when the cell is saturated with actin-binding proteins, an increase in actin filamentation will lead to an increase in the activation of actin-binding proteins. Nevertheless, in this scenario of increasing both the number of actin springs N_a and linker springs N_l, we again see similar trends as with increasing N_l but keeping N_a fixed.

To explain these variations, we hypothesize that there is only a single parameter—the network connectivity ξ—that governs how this random cytoskeleton network transduces mechanical stress to deform the nucleus. We define ξ to be the ratio of the number of springs (actin and linker) in uninterrupted paths to the total number of actin and linker springs. Thus, $0 \leq \xi \leq 1$. An uninterrupted path refers to a continuous chain of springs (actin and linker) that connects at least one point on the plasma membrane to at least one point on the nucleus membrane. A value of $\xi = 0$ means that the plasma and nucleus membranes are not connected by the cytoskeleton, whereas a value of $\xi = 1$ means that the all the springs play a role in the propagation of stresses from the plasma membrane to the nucleus membrane. Increasing the number of actin or linker springs or both will result in an increase in the network connectivity. This is shown in Fig. 6, which shows the monotonically increasing dependence of ξ on N_l and N_a.

Now, we can instead plot the nucleus strain and nucleus displacement as a function of network connectivity ξ regardless of how the numbers of springs (actin or linker) in the network change. This is shown in Fig. 7. We see that the curves for nucleus strain for both varying N_l and N_a collapse onto a master curve and similarly for the curves for nucleus displacement. Thus, network connectivity ξ can be regarded as the single parameter that governs mechanical stress propagation in the random cytoskeleton network.

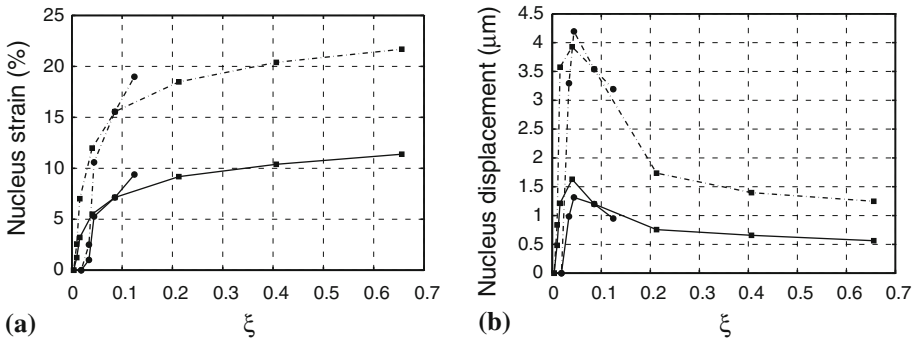

Fig. 7 **a** Nucleus strain and **b** nucleus displacement network connectivity ξ for pulling to 10 μm (*solid lines*) and 20 μm (*dash-dot lines*) and for varying the number of linker springs N_l (*squares*) and actin springs N_a (*circles*)

4 Discussion

To explain the dependences of the nucleus strain and nucleus displacement on network connectivity ξ, we can imagine that the whole three-dimensional random cytoskeleton network can be represented as a one-dimensional chain of nonlinear springs as sketched in Fig. 8a. In this one-dimensional model, the plasma and nucleus membranes and cytoskeleton are all modeled as nonlinear springs with stiffnesses k_p, k_n, and k_c, respectively. Mechanical stress σ is applied to one end of this model, while the opposite end is assumed to be fixed. For a given set of values for the following model parameter k_p, k_n, k_c, and σ, the nodal responses x_1, x_2, x_3, x_4, and x_5 can be computed analytically. We define the nucleus strain and displacement in this model to be $(x_3 - x_2)$ and x_2, respectively.

We argue that both k_c and σ depend on the network connectivity ξ in the manner depicted in Fig. 8b. First, the increase of k_c with ξ represents the increase in the elastic modulus of the network when its connectivity increases. In triangular lattice spring networks, this result is well known, where the network's elastic modulus increases nonlinearly with the fraction of bonds present (Feng and Sen 1984; Day et al. 1986). Furthermore, it has also been experimentally observed that the elastic modulus of in-vitro actin networks increases nonlinearly with both crosslinker density and actin concentration (Gardel et al. 2004). We note that our functional variation of k_c with ξ can be seen as a projection of the state diagram in Fig. 1a of Gardel et al. (2004) at a fixed value of actin concentration.

Second, the increase of σ with ξ can be justified by observing that, in our three-dimensional model, it is the strain, rather than the stress that is imposed externally in the form of a prescribed displacement boundary condition that is applied to the plasma membrane. This is to model the region of the plasma membrane that is attached to the micropipette and being pulled away from the cell until the specific displacement is obtained in the experiments of (Maniotis et al. 1997). The relationship between σ and ξ in our one-dimensional model (depicted in Fig. 8b) can be thought of as a correction to the boundary conditions in the one-dimensional model.

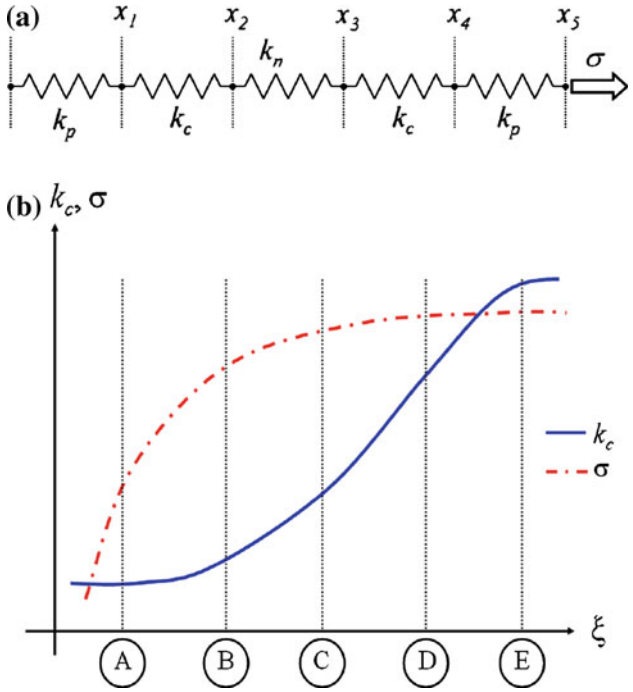

Fig. 8 **a** Representation of the three-dimensional random cytoskeleton network as a one-dimensional chain of nonlinear springs. The plasma and nucleus membranes and cytoskeleton are modeled as nonlinear springs with stiffnesses k_p, k_n, and k_c, respectively. Mechanical stress σ is applied to one end of this model, while the opposite end is assumed to be fixed. Nucleus strain and nucleus displacement are calculated as $(x_3 - x_2)$ and x_2, respectively. **b** The assumed functional variation of k_c (*solid line*) and σ (*dash-dot line*) with network connectivity ξ. The labels A to E refer to connectivity values discussed in the text

From a physical interpretation, we would intuitively expect the stress transmitted to the cytoskeleton network to be dependent on magnitude of the externally imposed strain, i.e., a higher imposed strain results in a higher stress being imposed on the cytoskeleton network. This is evident from the trend of the nucleus strain and nucleus displacement for different pulling distance (see Fig. 3). Similarly, we would also expect the stress, σ being transmitted to the cytoskeleton network to increase (for a given magnitude of the imposed strain) with increasing connectivity. This can be attributed

to the fact that as the network becomes more connected, the number of uninterrupted paths connecting the membrane to the nucleus increases. This new uninterrupted paths help facilitate the transmission of the imposed strain into stress being borne by the network. This response can be better understood if we consider this trivial scenario: Initially, only one uninterrupted path connects the nucleus membrane to the portion of the plasma membrane where the imposed strain is applied. Thus, the force on the nucleus is simply the force transmitted through this single path. Consider the effect of adding one new uninterrupted path between the nucleus and the membrane. In this case, the force on the nucleus will double. (We note that our approach for incorporating this force transmission effect through a functional variation in the applied mechanical stress is not unique. Another possible alternative is to prescribe a strain-dependent stiffness for the cytoskeleton spring in the one-dimensional model along with a prescribed displacement boundary condition.)

Solving for the nodal values x_1 to x_5 analytically, with the functional dependence of k_c and σ as discussed, we can indeed obtain the correct shapes of the curves for how nucleus strain and nucleus displacement vary with network connectivity, see Fig. 7. Therefore, we can interpret the effect of varying the number of linker springs as follows. For networks with a small number of linker springs, the connectivity is low. As more linker springs are added to the network, the network stiffens and the amount of stress transmitted to the nucleus increases (corresponding to points A to C in Fig. 8b). Both effects add up to an increase in nucleus strain and nucleus displacement. However, as more linker springs are added, the increase in network connectivity arises from the increased number of springs connecting to uninterrupted paths rather than an increase in the number of uninterrupted paths. Therefore, the effect of network stiffening dominates the increase in amount of stress transmission. (This is reflected in the decrease in the gradient of σ and the increase in the gradient of k_c from points C to E in Fig. 8b.)

Our modeling results so far have suggested that the connectivity of the random cytoskeleton network controls the propagation of mechanical stresses from the plasma membrane to the nucleus membrane. In the context of mechanotransduction, this suggests that alternations to the connectivity of the cytoskeleton can modulate changes in nucleus shape and gene expression resulting from external mechanical stimulus. We suggest that our model can be extended in the future to study the formation of stress fibers from single actin polymers. Then, we can study the experiments by Thery et al. (2006) that showed that the orientation of the stress fibers in stationary, nonmigrating cells is dependent on the shape of the fibronectin-coated micropattern that the cells adhered to. These micropatterns constrain the formation of focal adhesions to only certain regions of the substrate and therefore affects the orientation of the stress fibers formed between these focal adhesions. Since the cytoskeleton is mechanical coupled to the nucleus, it is conceivable that the shape and position of the nucleus is also dependent on the shape of these micropatterns. We propose that our model be used to investigate this dependency and to understand how substrate effects (through constraints on the location of focal adhesions) can be transmitted to changes in the nucleus shape and position.

Finally, we proposed that the results obtained from our model can be validated by using the experimental setup of laser ablation to sever a small number of actin filaments (Shen et al. 2005; Colombelli et al. 2009), thereby modifying the connectivity of the cytoskeletal network. The resultant changes in the nucleus shape and position arising from such a localized disruption in the cytoskeleton network can be measured experimentally. Similarly, we can use our three-dimensional model to predict these changes for a given disruption to the connectivity of the cytoskeleton network and compare our results to the experimental measurement. In addition, the comparison of the timescales of nucleus deformation measured experimentally and calculated computationally can also provide additional insights into the unresolved question as to whether biochemical signaling or mechanical coupling is the predominant mechanism in explaining nucleus shape changes upon external mechanical stimulus.

5 Conclusion

We have described a three-dimensional random network model of the cytoskeleton and have used it to study stress propagation from the plasma membrane to the nucleus membrane. We applied our model to study nucleus strain and displacement resulting from micropipette pulling applied on the plasma membrane (Maniotis et al. 1997). We showed that the results obtained from our simulation are in good agreement with the published experimental results. Next, we showed that the increasing the network connectivity causes the nucleus strain to increase in a sigmoidal manner and the nucleus displacement to exhibit a biphasic response. We explained these results qualitatively with the help of a one-dimensional chain of nonlinear springs.

In our model, we have neglected the effect of prestress in the cytoskeleton network and have assumed that the actin filaments are linear elastic. These can be implemented rather easily in future work. However, we do not expect the qualitative trends of our results to be dependent on the magnitude of the prestress or the exact form of the nonlinearity of the filament elasticity. We have also neglected the polymerization and depolymerization of the actin filaments, because the timescale of our simulation, on the order of ~ 10 s, is shorter than the remodeling timescale of the cytoskeleton network which is on the orders of minutes.

Acknowledgments We thank Kam W. Leong for insightful discussions.

References

Alberts B, Johnson A, Lewis J, Raff M, Roberts K, Walter P (2002) Molecular biology of the cell, 4th edn. Garland Science, New York

Caille N, Thoumine O, Tardy Y, Meister JJ (2002) Contribution of the nucleus to the mechanical properties of endothelial cells. J Biomech 35(2): 177–187

Chien S (2007) Mechanotransduction and endothelial cell homeostasis: the wisdom of the cell. Am J Physiol Heart Circ Physiol 292(3): H1209–H1214

Colombelli J, Besser A, Kress H, Reynaud EG, Girard P, Caussinus E, Haselmann U, Small JV, Schwarz US, Stelzer EHK (2009) Mechanosensing in actin stress fibers revealed by a close correlation between force and protein localization. J Cell Sci 122(Pt 10): 1665–1669

Crisp M, Liu Q, Roux K, Rattner JB, Shanahan C, Burke B, Stahl PD, Hodzic D (2006) Coupling of the nucleus and cytoplasm: role of the LINC complex. J Cell Biol 172(1): 41–53

Dalby M (2005) Topographically induced direct cell mechanotransduction. Med Eng Phys 27(9): 730–742

Dalby MJ, Riehle MO, Sutherland DS, Agheli H, Curtis ASG (2004) Use of nanotopography to study mechanotransduction in fibroblasts-methods and perspectives. Eur J Cell Biol 83(4): 159–169

Day AR, Tremblay RR, Tremblay AMS (1986) Rigid backbone: a new geometry for percolation. Phys Rev Lett 56(23): 2501–2504

Doddi SK, Bagchi P (2009) Three-dimensional computational modeling of multiple deformable cells flowing in microvessels. Phys Rev E Stat Nonlinear Soft Matter Phys 79(4 Pt 2):046,318

Engler AJ, Sen S, Sweeney HL, Discher DE (2006) Matrix elasticity directs stem cell lineage specification. Cell 126(4): 677–679

Evans EA, Skalak R (1979a) Mechanics and thermodynamics of biomembranes: part 1. CRC Crit Rev Bioeng 3(3): 181–330

Evans EA, Skalak R (1979b) Mechanics and thermodynamics of biomembranes: part 2. CRC Crit Rev Bioeng 3(4): 331–418

Feng S, Sen PN (1984) Percolation on elastic networks: new exponent and threshold. Phys Rev Lett 52(3): 216–219

Forgacs G (1995) On the possible role of cytoskeletal filamentous networks in intracellular signaling: an approach based on percolation. J Cell Sci 108(6): 2131–2144

Gardel ML, Shin JH, MacKintosh FC, Mahadevan L, Matsudaira P, Weitz DA (2004) Elastic behavior of cross-linked and bundled actin networks. Science 304(5675): 1301–1305

Gardel ML, Nakamura F, Hartwig J, Crocker JC, Stossel TP, Weitz DA (2006a) Stress-dependent elasticity of composite actin networks as a model for cell behavior. Phys Rev Lett 96(8):088,102

Gardel ML, Nakamura F, Hartwig JH, Crocker JC, Stossel TP, Weitz DA (2006b) Prestressed F-actin networks cross-linked by hinged filamins replicate mechanical properties of cells. Proc Natl Acad Sci USA 103(6): 1762–1767

Giannone G, Sheetz MP (2006) Substrate rigidity and force define form through tyrosine phosphatase and kinase pathways. Trends Cell Biol 16(4): 213–223

Gudi S, Nolan JP, Frangos JA (1998) Modulation of GTPase activity of G proteins by fluid shear stress and phospholipid composition. Proc Natl Acad Sci USA 95(5): 2515–2519

Guo W, Frey MT, Burnham NA, li Wang Y (2006) Substrate rigidity regulates the formation and maintenance of tissues. Biophys J 90(6): 2213–2220

Head DA, Levine AJ, MacKintosh FC (2003) Distinct regimes of elastic response and deformation modes of cross-linked cytoskeletal and semiflexible polymer networks. Phys Rev E Stat Nonlinear Soft Matt Phys 68(6 Pt 1):061,907

Huisman EM, van Dillen T, Onck PR, Vander Giessen E (2007) Three-dimensional cross-linked F-actin networks: relation between network architecture and mechanical behavior. Phys Rev Lett 99(20):208,103

Jean RP, Chen CS, Spector AA (2005) Finite-element analysis of the adhesion-cytoskeleton-nucleus mechanotransduction pathway during endothelial cell rounding: axisymmetric model. J Biomech Eng 127(4): 594–600

Kim T, Hwang W, Lee H, Kamm RD (2009) Computational analysis of viscoelastic properties of crosslinked actin networks. PLoS Comput Biol 5(7):e1000,439

Liu WF, Nelson CM, Tan JL, Chen CS (2007) Cadherins, RhoA, and Rac1 are differentially required for stretch-mediated proliferation in endothelial versus smooth muscle cells. Circ Res 101(5): e44–e52

Lo CM, Wang HB, Dembo M, Wang YL (2000) Cell movement is guided by the rigidity of the substrate. Biophys J 79(1):144–152

Maniotis AJ, Chen CS, Ingber DE (1997) Demonstration of mechanical connections between integrins, cytoskeletal filaments, and nucleoplasm that stabilize nuclear structure. Proc Natl Acad Sci USA 94(3): 849–854

Marcelli G, Parker KH, Winlove CP (2005) Thermal fluctuations of red blood cell membrane via a constant-area particle-dynamics model. Biophys J 89(4): 2473–2480

Martinac B (2004) Mechanosensitive ion channels: molecules of mechanotransduction. J Cell Sci 117(Pt 12): 2449–2450

Mastro AM, Babich MA, Taylor WD, Keith AD (1984) Diffusion of a small molecule in the cytoplasm of mammalian cells. Proc Natl Acad Sci USA 81(11): 3414–3418

Mederos y Schnitzler M, Storch U, Meibers S, Nurwakagari P, Breit A, Essin K, Gollasch M, Gudermann T (2008) Gq-coupled receptors as mechanosensors mediating myogenic vasoconstriction. EMBO J 27(23): 3092–3093

Na S, Collin O, Chowdhury F, Tay B, Ouyang M, Wang Y, Wang N (2008) Rapid signal transduction in living cells is a unique feature of mechanotransduction. Proc Natl Acad Sci USA 105(18): 6626–6631

Nalepa G, Harper JW (2004) Visualization of a highly organized intranuclear network of filaments in living mammalian cells. Cell Motil Cytoskelet 59(2): 94–108

Onck PR, Koeman T, van Dillen T, Van der Giessen E (2005) Alternative explanation of stiffening in cross-linked semiflexible networks. Phys Rev Lett 95(17):178,102

Palmer JS, Boyce MC (2008) Constitutive modeling of the stress–strain behavior of F-actin filament networks. Acta Biomater 4(3): 597–612

Sato M, Levesque MJ, Nerem RM (1987) An application of the micropipette technique to the measurement of the mechanical properties of cultured bovine aortic endothelial cells. J Biomech Eng 109(1): 27–34

Shafrir Y, Forgacs G (2002) Mechanotransduction through the cytoskeleton. Am J Physiol Cell Physiol 282(3): C479–C486

Shen N, Datta D, Schaffer CB, LeDuc P, Ingber DE, Mazur E (2005) Ablation of cytoskeletal filaments and mitochondria in live cells using a femtosecond laser nanoscissor. Mech Chem Biosyst 2(1): 17–25

Shin JH, Gardel ML, Mahadevan L, Matsudaira P, Weitz DA (2004) Relating microstructure to rheology of a bundled and cross-linked F-actin network in vitro. Proc Natl Acad Sci USA 101(26): 9636–9641

Stewart CL, Roux KJ, Burke B (2007) Blurring the boundary: the nuclear envelope extends its reach. Science 318(5855): 1408–1412

Tetsunaga T, Furumatsu T, Abe N, Nishida K, Naruse K, Ozaki T (2009) Mechanical stretch stimulates integrin alphaVbeta3-medi-

ated collagen expression in human anterior cruciate ligament cells. J Biomech 42(13): 2097–2103

Thery M, Pepin A, Dressaire E, Chen Y, Bornens M (2006) Cell distribution of stress fibres in response to the geometry of the adhesive environment. Cell Motil cytoskelet 63(6): 341–345

Thomas CH, Collier JH, Sfeir CS, Healy KE (2002) Engineering gene expression and protein synthesis by modulation of nuclear shape. Proc Natl Acad Sci USA 99(4):1972–1977

Tzima E, Irani-Tehrani M, Kiosses WB, Dejana E, Schultz DA, Engelhardt B, Cao G, DeLisser H, Schwartz MA (2005) A mechanosensory complex that mediates the endothelial cell response to fluid shear stress. Nature 437(7057): 426–431

Wang N, Tytell JD, Ingber DE (2009) Mechanotransduction at a distance: mechanically coupling the extracellular matrix with the nucleus. Nat Rev Mol Cell Biol 10(1): 75–82

Wiesner TF, Berk BC, Nerem RM (1997) A mathematical model of the cytosolic-free calcium response in endothelial cells to fluid shear stress. Proc Natl Acad Sci USA 94(8): 3726–3731